

High-precision method for measuring the photothermal properties of transparent media with digital holography

(Invited Paper)

David C. Clark and Myung K. Kim*

Digital Holography and Microscopy Laboratory, Department of Physics, University of South Florida, 4202 E. Fowler Avenue, Tampa, Florida 33620, USA

*Corresponding author: mkkim@usf.edu

Received August 26, 2011; accepted September 15, 2011; posted online November 18, 2011

Quantitative phase microscopy by digital holography provides direct access to the phase profile of a transparent subject with high precision. This is useful for observing phenomena that modulate phase, but are otherwise difficult or impossible to detect. In this letter, a carefully constructed digital holographic apparatus is used to measure optically induced thermal lensing with an optical path difference precision of less than 1 nm. Furthermore, by taking advantage of the radial symmetry of a thermal lens, such data are processed to determine the absorption coefficient of transparent media with precisions as low as $1 \times 10^{-5} \text{ cm}^{-1}$ using low power (30 mW) continuous wave (CW) excitation.

OCIS codes: 090.0090, 090.1995, 350.6830.

doi: 10.3788/COL201109.120001.

When a beam of incident light passes through a medium, that medium may absorb some energy of the beam. This absorbed energy causes a change in temperature of the absorbing region of the media, which diffuses to other parts of the medium in a way described by its thermal properties. Since the index of refraction is a temperature dependant property, the temperature gradient results in a refractive index gradient and, therefore, an optical path difference. This effect is referred to as thermal lensing and has been the focus of many other studies as an indicator of the optical and thermal properties of materials^[1–3].

Due to the change in optical path length, a resulting phase shift can be detected at a plane on the far side of the medium. The description of this result can be simplified if the dimensions of the sample are such that the edge effects and container medium can be ignored relative to the effects in the sample medium itself. Such a model has previously been developed, and is known as the two-dimensional (2D) infinite model^[4]. This model mathematically relates the resulting phase shift to the photothermal properties of the medium in a focused continuous wave (CW) excitation laser beam and an unfocused or collimated imaging beam, such as that used in this letter.

The validity of the 2D infinite model is based on several assumptions, and the experimental design should take these into account. The sample cell path length should be comparable to the confocal parameter (twice the Rayleigh range) of the excitation beam to ensure that the spot size remains relatively constant through the sample. In addition, the sample cell dimensions should be large compared with the excitation beam radius so that both radial and axial edge effects can be ignored. The sample should absorb very little power to avoid convection effects. Finally, the temperature coefficient of the refractive index, $\frac{dn}{dT}$, should be constant in the range of temperatures observed. With these assumptions in mind, the laser-induced change in temperature within the sample can be described. Using expressions for the heat gen-

erated in a sample by a Gaussian excitation beam and the corresponding solution to the heat transfer equation, a previous study^[4] has derived the following relation:

$$\Delta T(r, t) = \frac{2P\alpha}{\pi c\rho w^2} \int_0^t \frac{1}{1 + 2t'/\tau} \exp\left(-\frac{2r^2/w^2}{1 + 2t'/\tau}\right) dt', \quad (1)$$

where r is the radial distance from the beam axis; t is the time of exposure to the excitation beam; P is the total excitation beam power at the sample; α , c , and ρ are the absorption coefficient, specific heat and density of the sample, respectively; w is the excitation beam radius in the sample. The characteristic thermal time constant, τ , is given by $\tau = \frac{w^2 c\rho}{4\kappa}$ with thermal conductivity, κ . The resulting refractive index gradient can be described by

$$n(r, t) = n_0 + \frac{dn}{dT} \Delta T(r, t), \quad (2)$$

where n_0 is the index of refraction at the starting temperature of the sample. This leads directly to phase shift described by

$$\begin{aligned} \phi &= \frac{2\pi}{\lambda} l [n(r, t) - n(0, t)] \\ &= \frac{2\pi}{\lambda} l \frac{dn}{dT} [\Delta T(r, t) - \Delta T(0, t)], \end{aligned} \quad (3)$$

where λ is the wavelength of the probe beam, and l is the thickness of the sample. Substituting Eq. (1) into Eq. (3), the phase shift can be rewritten as

$$\phi = \theta \int_0^t \frac{1}{1 + 2t'/\tau} \left[1 - \exp\left(-\frac{2r^2/w^2}{1 + 2t'/\tau}\right) \right] \frac{dt'}{\tau}, \quad (4)$$

where

$$\theta = -\frac{P\alpha l (dn/dT)}{\kappa \lambda}. \quad (5)$$

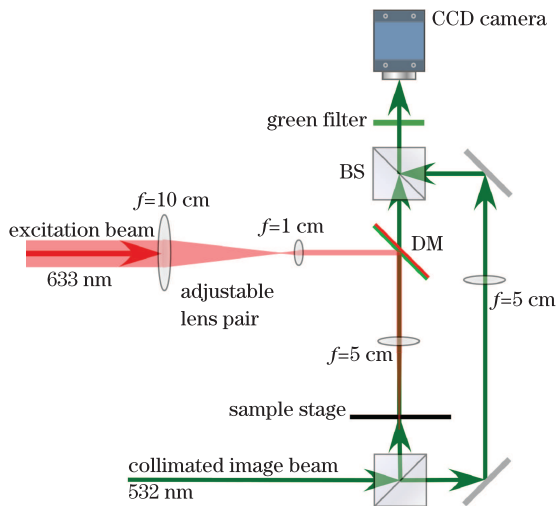


Fig. 1. (Color online) Experimental apparatus. The excitation beam (red) is reflected downward by the DM through the sample by the probe-shared objective lens. The probe beam (green) is the object arm of the MZI, which passes upward through the sample, combines with the reference beam, and creates the hologram captured by the CCD camera.

Previous experimental methods have been developed to approximate this phase shift and then used to measure very low absorption coefficients of materials, demonstrating good agreement with expected values through a far-field diffraction technique^[1,2]. These methods require additional mathematical approximation and fitting to determine the change in the wavefront of the incident beam and, therefore, the phase shift resulting from the thermal lens. Since digital holography is a phase imaging method^[5,6], this phase shift can be directly measured, without further approximations, following a process similar to photothermal interferometry^[7]. In addition, there is no necessary minimum distance from the thermal lens to the detector plane when measuring by digital holography. Our previous work has shown that improved accuracy and precision over these traditional methods is achieved through the use of digital holography^[3]. In this letter, we describe our use of quantitative phase microscopy by digital holography (DH-QPM) in a high precision method to map the thermal lens and measure the absorption coefficient of transparent media using low excitation power. The goal of this study is to maximize the use of the data collected by an optimized system to achieve improved measurement precision with standard optical laboratory components.

Figure 1 shows a diagram of the experimental apparatus. We used a Mach-Zehnder interferometer (MZI) to create the hologram of the sample using low power (~ 1 mW) 532-nm laser light. In the experiment, the imaging beam arrived collimated at a beam splitter (BS) that then transmitted half the beam into the reference arm and reflected half the beam into the object arm of the setup. The beams each followed a similar path (through matching singlet objective lenses) before recombining through another BS, with the main difference being that the object beam had passed through the sample area of the interferometer. The interference of the phase-modulated object beam with the reference beam created the hologram, which was recorded by a digital

CCD camera placed atop the setup and passed into our LabVIEW personal computer platform for amplitude and phase reconstruction based on the angular spectrum method^[8].

An integrated optical excitation arm delivered a 30-mW, 632.8-nm CW laser beam to the system. Afterwards, the beam passed through a 10:1 focal length lens pair to create a much reduced beam radius. A dichroic mirror (DM) reflected this excitation beam down toward the sample while allowing the probe beam to transmit up toward the CCD camera. The excitation beam passed through the shared objective lens, which in turn, focused the already thin beam through the sample area. The objectives were chosen to have long effective focal lengths in order to meet the requirements of the 2D infinite model described above. A removable green bandpass filter was placed just in front of the CCD camera to filter out any 632.8-nm excitation light leaking through the DM. This “leaky” light, however, can be used to profile the excitation beam by temporarily removing the green filter. The excitation beam radius, w , is defined as the radius at which the Gaussian beam intensity is reduced to e^{-2} of its maximum. With the green filter in place, a hologram containing complete phase and amplitude information was captured by the CCD camera and processed by our software routines. This process reconstructed the phase image both with and without excitation.

The sample consisted of a pure liquid in a glass cuvette ($5 \times 10 \times 45$) with a sealable lid. With the excitation beam profiled and adjusted to a desired radius using the excitation arm lenses, the sample was placed on the sample stage on its side oriented with a 5-mm path length. The sample stage can be adjusted in z to optimize the location of the sample for the desired beam radius. At this time, all general phase aberrations, including wavefront curvature mismatch, can be easily compensated by storing a background phase image and subtracting this from subsequent images. While viewing the baseline phase image shown in Fig. 2(a), the optical excitation beam was turned on and a thermal lens became visible, as demonstrated in Fig. 2(b).

Our previous work has demonstrated excellent temporal and spatial agreement with the 2D infinite model^[9]. Therefore, in this letter, we used optically triggered timing to capture the data at precisely 4 000 ms after excitation begins, with a shutter speed of less than 100 μ s.

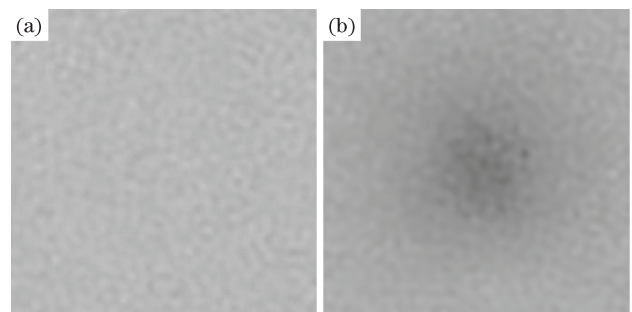


Fig. 2. Example phase maps of a sample with (a) no excitation and (b) optical excitation resulting in a thermal lens (higher power excitation was used here to improve structure visibility for print). Phase shift is represented as dark for smaller values and light for higher values. Field of view is 100 μ m.

Table 1. Experimental Parameters for Benzyl Alcohol

Parameter	Symbol	Value
Power (mW)	P	30
Excitation Beam Radius (μm)	w	70
Probe Beam Wavelength (nm)	λ	532
Sample Cell Path Length (mm)	l	5.0
Excitation Duration (s)	t	4.000
Refractive Index (20°C) ¹	n_0	1.540
Thermal Conductivity ¹ (W/(m·°C))	k	0.159
Specific Heat Capacity ¹ (J/(g·k))	c	2.02
Density ¹ (g/ml)	ρ	1.044
Thermal Time Constant (ms)	τ	16.2
Temp. Coefficient of RI ² (°C ⁻¹)	dn/dT	-3.5×10^{-4}
Absorption Coefficient (cm ⁻¹)	α_{exp}	$(6.4 \pm 0.1) \times 10^{-4}$

¹CRC Handbook of Chemistry and Physics, 2008.

²El-Kashef, Hassan, and El-Ghazaly, App. Opt. 33, 3540 (1994).

At this time, the rate of change of thermal lens phase signal significantly reduced (~ 0.001 rad/s); thus, any error from our timing mechanism would be negligible.

Table 1 indicates the experimental parameters of benzyl alcohol, a transparent liquid. The absorption coefficient at 632.8 nm, α_{exp} , was determined experimentally to be $(6.4 \pm 0.1) \times 10^{-4}$ cm⁻¹ as described herein. By taking a single cross-section through the center of the thermal lens structure in the phase map, a profile of the thermal lens phase signal versus position was obtained as shown in Fig. 3. While this raw data demonstrates an impressive precision (better than ± 0.01 rad), it does not adequately represent the large amount of data collected by this method.

In order to maximize the use of the 2D array of data, we consider the radial symmetry of the structure being measured. The center of the thermal lens was determined by locating the X- and Y-minima, after which a suitable radius was selected. A simple algorithm averaged the phase data around the circumference of the circle for each radial distance to produce a one-dimensional (1D) array of averaged phase values versus radial distance. We used 100 points around the circumference for averaging. This result is plotted in Fig. 4, along with the model prediction

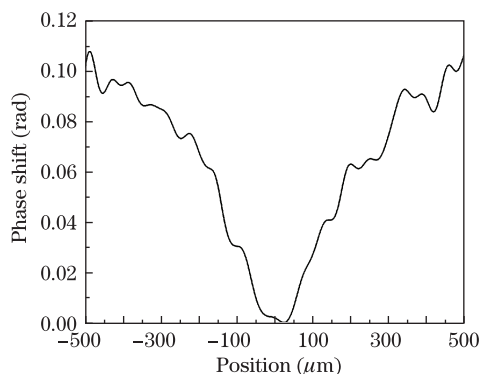


Fig. 3. Single cross-section through center of the thermal lens phase structure.

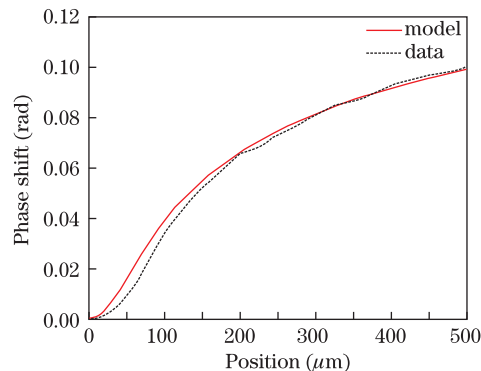


Fig. 4. Phase shift versus radial distance from the center of excitation beam for experimental data (dotted) and model predictions (solid) for a thermal lens in benzyl alcohol. Shift at the origin is set to zero as a reference to the rest of the thermal lens.

using the experimentally determined absorption coefficient. Although the deviation is very small, we note here that there is greater deviation toward the center of the structure where the model assumes a constant excitation beam radius through the sample. Certainly, this is not actually true for a focused excitation beam and this small difference is detectable by the current method. The data taken at a sufficient distance from this artifact (in this case, 170 μm or further from the origin) never deviates more than 0.002 rad from the model prediction.

We display the entire radial path here to demonstrate the strength of the relationship between the experiment and the model; however, determining the absorption coefficient only requires the selection of a single radial location. The most suitable selection is typically the farthest distance from the center of the thermal lens structure that still allows complete circular averaging. However, as demonstrated, many selections are available with little or no consequence. Additionally, if the raw data are particularly noisy, the number of points around the circle for averaging can be increased (within the confines of the data array size).

The noise levels of our system were mathematically determined between each measurement by phase imaging the sample, with no excitation beam present and by taking the standard deviation of the raw single cross-section to indicate background noise. Values ranged between 0.003 and 0.015 rad, with 0.01 rad as the average. In addition to the determination of absorption coefficient, the phase shift caused by a thermal lens has a direct mathematical relationship with shifts in temperature, index of refraction, and optical path length of the media as described by Eq. (3). As such, a direct measurement of the phase shift yields these parameters with similar relative precision. By substituting the current typical noise level of our system (0.01 rad) into Eq. (3) and solving for the temperature shift difference, the absolute difference in temperature between any two points can be determined to a precision of 0.0005 K. Similarly, the shift in refractive index is determined with 1.7×10^{-7} precision. Optical path difference is described by $l(\Delta n)$, where l is our cuvette path length (5 mm), and Δn is the refractive index difference. Therefore, at the current typical noise level, this system determines the

optical path difference with a typical 0.8-nm resolution. Although these values of precision are based on the noise level of the system, the symmetry in this study permits improvement by almost an order of magnitude, using the averaging method described above.

In conclusion, through careful optimization of the DH-QPM apparatus using standard optics laboratory components, we demonstrate the measurement of photothermal properties of pure substances with high precision. The currently described method can be immediately useful as a valuable tool in various analytical chemistry applications requiring high sensitivity^[10–12]. In fact, DH-QPM is capable of a full armory of such measurement through robust adaptability to alternative compact apparatus.

This work was supported in part by the National Science Foundation of USA under Grant No. 0755705.

References

1. A. Marcano O., C. Loper, and N. Melikechi, *Appl. Phys. Lett.* **78**, 3415 (2001).
2. H. Cabrera, A. Marcano, and Y. Castellanos, *Condens. Matter Phys.* **9**, 385 (2006).
3. D. C. Clark and M. K. Kim, *Appl. Opt.* **50**, 1668 (2011).
4. J. Shen, R. D. Lowe, and R. D. Snook, *Chem. Phys.* **165**, 385 (1992).
5. E. Cuche, F. Bevilacqua, and C. Depeursinge, *Opt. Lett.* **24**, 291 (1999).
6. C. Mann, L. Yu, C.-M. Lo, and M. Kim, *Opt. Express* **13**, 8693 (2005).
7. S. D. Woodruff and E. S. Yeung, *Anal. Chem.* **54**, 1174 (1982).
8. L. Yu and M. K. Kim, *Opt. Lett.* **30**, 2092 (2005).
9. D. C. Clark and M. K. Kim, *Proc. SPIE* **7908**, 79080T (2011).
10. W. S. Pegau, D. Gray, and J. R. V. Zaneveld, *Appl. Opt.* **36**, 6035 (1997).
11. M. Babin, D. Stramski, G. M. Ferrari, H. Claustre, A. Bricaud, G. Obolensky, and N. Hoepffner, *J. Geophys. Res.* **108**, 3211 (2003).
12. S. M. Colcombe, R. D. Lowe, and R. D. Snook, *Anal. Chim. Acta.* **356**, 277 (1997).